JOC The Journal of Organic Chemistry

Article

pubs.acs.org/joc

p-Quaterphenyls Laterally Substituted with a Dimesitylboryl Group: A Promising Class of Solid-State Blue Emitters

Guang-Liang Fu,[†] Hong-Yu Zhang,[‡] Yi-Qiao Yan,[†] and Cui-Hua Zhao*,[†]

[†]School of Chemistry and Chemical Engineering, Shandong University, Shanda Nanlu 27, Jinan 250100, P. R. China

[‡]State Key Laboratory of Supramolecular Structure and Materials, College of Chemistry, Jilin University, Changchun 130012, P. R. China

S *Supporting Information*

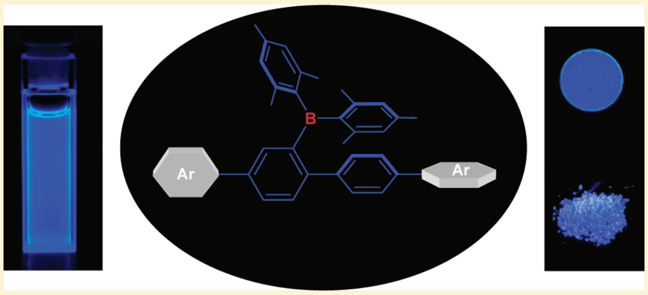

ABSTRACT: A new family of *p*-quaterphenyls **1**–**6** laterally substituted with a bulky electron-accepting dimesitylboryl group has been designed and synthesized. These compounds were characterized by X-ray crystallography, UV–vis and fluorescence spectroscopy, and DFT calculations as well as thermogravimetric analysis (TGA), differential scanning calorimetry (DSC), and cyclic voltammetry (CV). X-ray single-crystal analysis revealed that the *p*-quaterphenyl main chain framework exhibits a twisted structure due to the steric effect of the lateral boryl group, and the intermolecular interactions are effectively suppressed in the solid state. Despite the significantly twisted main-chain structure, these molecules still display efficient intramolecular charge-transfer emissions with large Stokes shifts. An intriguing finding is that all these molecules show bright fluorescence with good to excellent quantum yields in the blue region in the solid state. In addition, the two representative *p*-quaterphenyls **3** and **4** containing both the electron-accepting boryl group and the electron-donating carbazolyl (**3**) or diphenylamino group (**4**) possess high thermal stability and good oxidation–reduction reversibility, which together with their excellent solid-state fluorescence efficiency make them promising bipolar transporting blue emitters.

INTRODUCTION

Since the breakthrough discovery of organic electroluminescence (EL) by Tang and VanSlyke,[1] the organic light emitting diodes (OLEDs) employing organic fluorophores as emitters have attracted considerable interest because of their potential applications in flat panel displays[2] and solid-state lighting.[3] In OLEDs, organic emitters are used as thin films and thus the external quantum efficiency of the devices is greatly dependent on the fluorescence quantum yield of the emissive materials in the solid state. However, most organic fluorophores are highly emissive only in the dilute solution and tend to show a decrease of fluorescence efficiency in the solid state due to the severe fluorescence quenching, which may result from the intermolecular electronic interactions such as aggregate or excimer formation and energy migration in the solid state. As a result, in contrast to the great number of molecules that are known to be highly emissive in solution, the examples of highly emissive organic solids with a fluorescence quantum yield close to unity are still quite limited,[4] especially those exhibiting strong solid-state blue emission. It is even more challenging to achieve stable and efficient solid-state blue emitters compared with green and red emitters because of the relatively high energy gap required between the interactive orbitals, which may cause either poor photostability or low quantum efficiency.[5] However, blue is one of the primary colors (red, green, and blue) that are essential for the realization of a full-color display. In addition, blue-emitting materials may act as host materials for green and red dopants. In this context, it is of particular interest to develop blue emissive materials exhibiting high fluorescence efficiency in the pure solid state.

To achieve an intense solid-state emission, several effective strategies have been adopted, such as protection with bulky substituents,[6] cross dipole stacking,[7] taking advantage of aggregation-induced emission,[8–10] J-aggregate formation,[11] spiro concept[12] and enhanced intramolecular charge transfer (CT) transition.[13–15] Among them, we and others recently focused our attention on an interesting molecular design, in which the bulky electron-accepting dimesitylboryl groups[16] were introduced at the lateral positions of electron-donating π-conjugated framework.[13] This effective molecular design is attributed to two factors of the lateral dimesitylboryl group. One is the steric bulkiness that can prevent an intermolecular interaction. The other is the electron-accepting character that induces an intramolecular CT transition with a large Stokes shift and thus effectively suppresses self-quenching in the condensed state. The utility and generality of this molecular design have been demonstrated by synthesizing two series of compounds, 2,5-diborylphenylene-cored oligo(phenylenethynylene) systems and 3-boryl-2,2′-bithiophene

Received: December 20, 2011
Published: January 18, 2012

dx.doi.org/10.1021/jo202574n | *J. Org. Chem.* 2012, 77, 1983–1990

systems.[13] In the above two series of compounds, it was hard to attain ideal blue emissive molecules, especially those possess bipolar transporting properties, as a result of the extended conjugation of the parent π-framework. To continue our effort in the development of highly solid-state emissive materials utilizing boron element, we herein disclose another series of π-conjugated system laterally substituted with a bulky electron-accepting boryl group, *p*-quaterpheyls **1**−**6** containing 2-dimesitylboryl-4,4′-biphenylene as a core unit (Figure 1). The *p*-quaterpheyl was chosen as the parent framework because of its limited conjugation, which was expected to prevent the emission from red-shifting. It was intriguing to find that these boryl-substituted *p*-quaterphenyls exhibit intense solid-state fluorescence with the quantum yields close to unity in the blue region, even those containing strong electron-donating carbazolyl or diphenylamino groups. Their single-crystal X-ray structure, photophysical properties in solution and the solid state, theoretical calculations, thermal stabilitie, as well as electrochemical properties have been comprehensively characterized to investigate the characteristics of the current π-conjugated system and the impact of the structure modification.

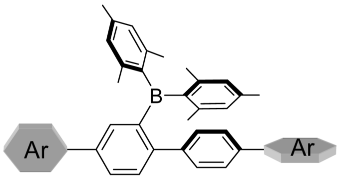

1: Ar = Ph
2: Ar = *p*-MeOC$_6$H$_4$
3: Ar = *p*-CarbazolylC$_6$H$_4$
4: Ar = *p*-Ph$_2$NC$_6$H$_4$
5: Ar = *o*-Ph$_2$NC$_6$H$_4$
6: Ar = *m*-Ph$_2$NC$_6$H$_4$

Figure 1. Structures of boryl-substituted *p*-quaterphenyls.

RESULTS AND DISCUSSION

Synthesis. The *p*-quaterphenyl derivatives **1**−**6** were prepared in two steps from 4,4′-dibromo-2-iodobiphenyl **7**,[17] as illustrated in Scheme 1. Thus, the selective monolithiation of **7** with *n*-BuLi at −78 °C followed by treatment with dimesitylfluoroborane afforded the borylated product **8** in 51% yield. With the precursor **8** in hand, the following Pd(0)-catalyzed Suzuki−Miyaura cross-coupling reaction with a variety of substituted phenylboronic acid proceeded smoothly to produce the boryl-substituted *p*-quaterphenyls **1**−**6** in good to excellent yields, with the exception of **5**. It is generally preferable to employ alternative methods such as Stille or Negishi coupling rather than Suzuki coupling when the substrate contains a triarylboron group,[18,13b] due to the association of hydroxide with the boron center, which makes the triarylboron compound susceptible to react in much the same manner as traditional aryl boronate to produce coupling product of its pendant aryl groups.[19] The success of the Suzuki coupling reaction of **8** with a variety of substituted phenylboronic acid is probably ascribed to the significant steric congestion of the boron center in it, which can prevent the attack of hydroxide. It is reasonable that the reaction of **8** with *o*-(diphenylamino)phenylboronic acid proceeded in a much lower yield relative to other substituted phenylboronic acids, considering the significant steric bulk of the diphenylamino group at the *o*-position. All of the obtained boryl-substituted π-conjugated compounds are stable in air and water and can be purified by silica gel column chromatography. They were fully characterized using ^{1}H and ^{13}C NMR spectroscopy and high-resolution mass spectrometry.

Scheme 1. Synthesis of Boryl-Substituted *p*-Quaterphenyls[a]

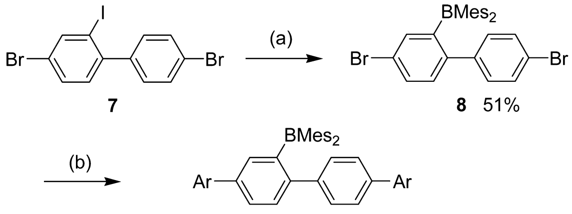

1: Ar = Ph (96%)
2: Ar = *p*-MeOC$_6$H$_4$ (80%)
3: Ar = *p*-CarbazolylC$_6$H$_4$ (73%)
4: Ar = *p*-Ph$_2$NC$_6$H$_4$ (70%)
5: Ar = *o*-Ph$_2$NC$_6$H$_4$ (19%)
6: Ar = *m*-Ph$_2$NC$_6$H$_4$ (75%)

[a] Reagents and conditions: (a) (i) *n*-BuLi, −78 °C, 1 h; (ii) Mes$_2$BF, THF, −78 °C to rt; (b) ArB(OH)$_2$, Pd(PPh$_3$)$_4$, Na$_2$CO$_3$ (2 M), toluene, reflux.

X-Crystal Structure Analysis. Among the newly prepared molecules, the structure of **2** was determined by single-crystal X-ray diffraction analysis (XRD). The crystals for XRD were obtained by recrystallization from a mixed solvent of CH$_2$Cl$_2$ and hexane. The molecular structure and packing structure of **2** are shown in Figure 2. In this compound, the trivalent boron centers are well protected by the methyl groups at the *o*-positions of two mesityl groups, which accounts for its high stabilities. It is noteworthy that the *p*-quaterphenyl main chain framework exhibits a significantly twisted structure, similar to other π-conjugated compounds laterally substituted with dimesitylboryl groups.[13] All of the benzene rings of the main chain are nonplanar with each other. The dihedral angle between benzene rings 1 and 2 is 28.7°. And the benzene ring 3 is twisted by a much larger dihedral angle (63.9°) relative to the benzene ring 2 due to the higher steric congestion between them. It is also interesting to note that the benzene ring 4 is further twisted relative to the benzene 3 with a dihedral angle of 45.7°, which is even larger than that between the benzene rings 1 and 2. Apparently, the significantly twisted conformation of the main-chain framework arises from the steric hindrance of the lateral dimesitylboryl group. Presumably due to the nonplanar structure of the main chain framework and the

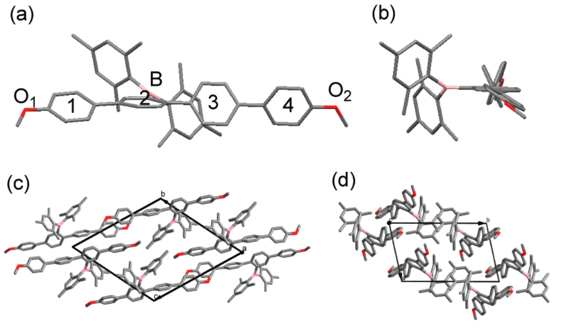

Figure 2. Crystal structure of **2**: (a), (b) the molecular structure and the packing structure; (c) view from *a* axis; (d) view from *c* axis. Hydrogen atoms are omitted for clarity.

steric bulkiness of the lateral dimesitylboryl group, the molecules are far apart from each other. The distance between the central 2 benzene planes of the two adjacent molecules is 6.39 Å, which is supposedly large enough to prevent intermolecular electronic interactions. Compounds **1**, **3**, and **4** would possibly exhibit similar main chain structure to that of **2** because of their similarities in the molecular structure and the main chains of **5** and **6** would presumably become much more twisted due to the increased steric hindrance induced by the lateral diphenylamino groups.

Photophysical Properties in Benzene Solutions. The UV/vis absorption and emission spectra of **1**−**6** in solutions were measured in benzene, which are shown in Figure 3. The corresponding data are summarized in Table 1.

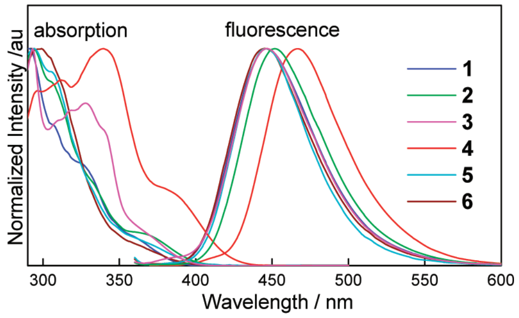

Figure 3. Absorption and fluorescence spectra of boryl-substituted *p*-quaterphenyls **1**−**6** in benzene.

Table 1. UV/Vis Absorption and Fluorescence Data for Boryl-Substituted *p*-Quaterphenyls 1−6 in Benzene

	absorption		fluorescence	
	λ_{abs} (nm)[a]	ε (M^{-1} cm^{-1})	λ_{em}[b] (nm)	Φ_F[c]
1	290	43000	449	0.51
2	373 (sh)	7280	456	0.64
3	370 (sh)	9910	451	0.62
4	384 (sh)	14550	469	0.60
5	301	49490	450	0.17
6	301	96650	449	0.32

[a] Only the longest maxima are shown. [b] Excited at the longest absorption maxima. [c] Calculated using quinine sulfate as standard.

In the absorption spectra, compounds **2**−**4** feature a weak shoulder band at the wavelength longer than that of the intense band, while this shoulder band is hard to distinguish for **1**. In addition, the shoulder band of **4** is much red-shifted relative to those of **2** and **3** (λ_{abs} = 373 nm for **2**, 370 nm for **3**, and 384 nm for **4**). The shoulder band of **2**−**4** is presumably assigned to the intramolecular charge-transfer (CT) transition from the HOMO delocalized over the whole π-conjugated framework to the LUMO mainly localized on the borylphenylene moiety. The trend observed in the absorption may be rationalized by considering that the HOMO energy levels of the present systems are highly dependent on electron-donating ability of the substituents at terminal positions. As the electron-donating ability of the terminal groups increases, the HOMO energy levels increase, leading to the intramolecular CT transition at the longer wavelength. As a result, the intramolecular CT absorption of the nonsubstituted *p*-quaterphenyl **1** is presumed to be blue-shifted relative to those of the electron-donating groups substituted **2**−**4** and thus possibly overlaps with the tail of the intense absorption band at the shorter wavelength. It is noteworthy the intramolecular CT transition bands were also not observed in the absorption spectra of **5** and **6**, the regioisomers of **4** with diphenylamino groups at different positions, indicating that the substituted sites of the electron-donating groups significantly affect the electronic structure of the present *p*-quaterphenyl systems.

In the fluorescence spectra, the boryl-substituted *p*-quaterphenyls **1**−**4** exhibit intense blue fluorescence with quantum yields ranging 0.51−0.64. The emission maximum wavelength is red-shifted with the increase in the electron-donating ability of the terminal *p*-substituents, from 449 nm for **1** to 469 nm for **4**. The bathochromism in the absorption and emission spectra from nonsubstituted **1** to the electron-donating Ph_2N substituted **4** is much less significant compared with other π-conjugated systems containing lateral dimesitylboryl groups.[13a,b] This phenomenon is presumably ascribed to the significant nonplanar main chain framework, which would prevent the participation of the *p*-substituents in the π-conjugation extension. Again the emissions of **5** and **6** are greatly blue-shifted by ca. 20 nm relative to that **4**, which are almost same to that of **1**. Moreover, **5** and **6** display much lower fluorescence quantum efficiency compared with that of **4** (Φ_F = 0.60 for **4**, 0.17 for **5**, 0.32 for **6**), confirming the substitution pattern has significant influence on the electronic structure, producing obviously different optical properties. Another noticeable feature for the present boryl-substituted *p*-quaterphenyls is the large Stokes shift for this quaterphenyl unit with such a limited conjugation length. There are almost no overlaps between the absorption and emission for all the derivatives, which may partially arises from significant structure differences between the twisted structure in the ground state and the presumably planar structure in the excited state.

Theoretical Studies. To elucidate the influence of the electronic effect and the substitution pattern of the substituents on the terminal benzene rings on the electronic structures and thus the photophysical properties, we conducted theoretical calculations of the representative derivatives, nonsubstituted **1**, electron-donating Ph_2N geometrically substituted **4**−**6**. The optimizations of the molecular geometry and total energy calculations were carried out using density functional theory (DFT) calculations at B3LYP/6-31G(d) level of theory. We also performed time-dependent density-functional theory (TD-DFT) calculations of these compounds at the B3LYP/6-31G(d) theory. The pictorial drawing of their molecular orbitals and the Kohn−Sham HOMO and LUMO energy levels are shown in Figure 4.

The nonsubstituted compound **1** has a HOMO delocalized over the entire *p*-quaterphenyl framework despite its twisted main chain structure, and its LUMO is localized on the central boryl-biphenylene moiety. The HOMO and LUMO energy levels are −5.60 and −1.64 eV, respectively. The calculated first excited state, mainly consisting of a HOMO→LUMO intramolecular CT transition, has an excitation energy of 3.33 eV (372 nm) with a small oscillator strength of 0.0801. The incorporation of the electron-donating Ph_2N groups at 4,4‴-positions of this skeleton (**4**) leads to a remarkable increase in the HOMO energy level by 0.76 eV, whereas the LUMO level remains almost unchanged. Consequently, the calculated first excited energy of **4** is reduced to 2.86 eV (434 nm). It is notable that the HOMO of **4** spreads over the entire quaterphenyl framework, including the Ph_2N unit. This change leads to a significant increase in the oscillator strength of the

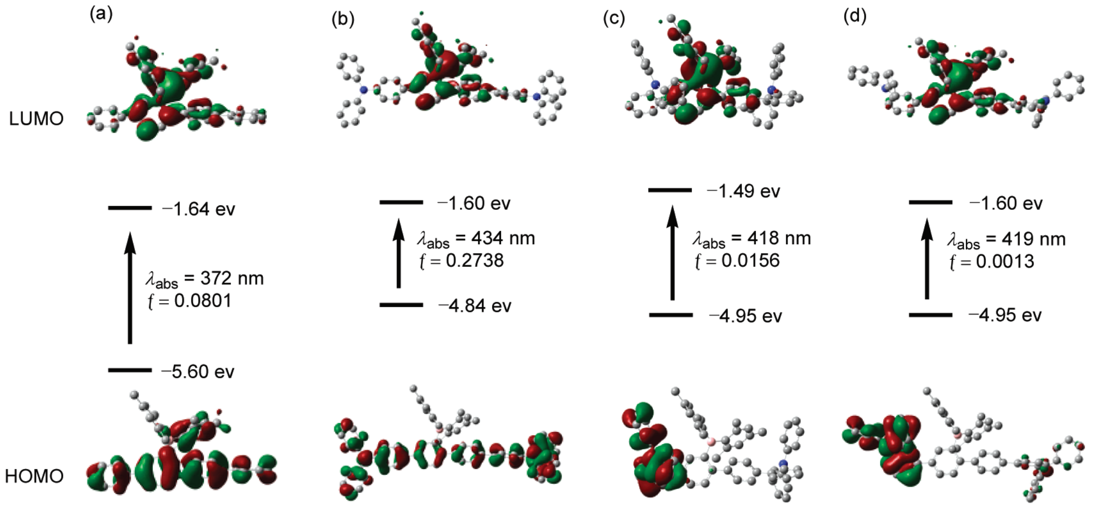

Figure 4. Plot of the Kohn−Sham HOMO and LUMO energy levels and pictorial drawings of the HOMOs and LUMOs for (a) **1**, (b) **4**, (c) **5**, and (d) **6**. The transition energies and oscillator strengths were calculated at the B3LYP/6-31G(d) level of theory.

first excited state (f = 0.2738). In contrast to the extended conjugation of the HOMO in **4**, the HOMO is mainly localized on the (diphenylamino)phenyl moiety which is located at the *meta*-position of the boryl group when the electron-donating Ph_2N groups are introduced at 2,2‴-positions (**5**) or 3,3‴-positions (**6**) of the quaterphenyl framework. As a consequence, both their HOMO energy levels are lowered by ca. 0.11 eV and the excitation energy of the first excited state is increased by ca. 0.11 eV compared to those of **4**. In conjunction with these changes, the oscillator strength of the first excited state decreases to 0.0156 and 0.0013 for **5** and **6**, respectively. Probably due to the quite low oscillator strength of **1**, **5**, and **6**, the lowest intramolecular charge-transfer transition bands are too weak to be distinguished in their absorption spectra. Whereas the accuracy of the calculated excitation energy is not sufficiently high by this level of calculations, these calculated results clearly demonstrate the nature of the transition significantly depends on electronic effect of the substituents and the substitution pattern of the molecular structure. The introduction of the electron-donating groups at 4,4‴-positions leads to the most effective conjugation and thus the most efficient intramolecular CT transition for this boryl-substituted *p*-quaterphenyl π-conjugated system, which is consistent with our experimental results.

Fluorescence Solvatochromism. To gain a deeper insight into the effect of the substituents on the intramolecular CT transitions and the excited states, we investigated the solvent effects in the absorption and emission spectra for **1**, **4**−**6**, the data for which are summarized in Table 2.

The fluorescence spectra of all these molecules show obvious solvatochromism while the absorption spectra display trivial solvent dependence (see the Supporting Information), indicating that they have more polar structures in the excited state relative to those in the ground state. To compare the degree of the polarization in the excited state among these molecules, we employed the Lippert−Mataga equation. (eq 1), in which C is a constant, μ_e and μ_g are the dipole moments in the excited state and ground state, respectively, and $\Delta\nu$ is the Stokes shift. Δf is the solvent polarity and is given by eq 2, in which ε is the dielectric constant and n is the optical refractive constant. Although this equation originally assumes the presence of a molecular dipole, it has been demonstrated to be applicable to several quadrupole extended π-conjugated molecules.[20,13d] For the present *p*-quaterphenyl derivatives and **4**−**6**, we indeed obtained linear relationships for the plots $\Delta\nu$ as a function of the Δf, as shown in Figure 5. The slope obtained for **4** is 8856 cm^{-1}, which is much steeper than that of **1** (2447 cm^{-1}). These results suggest a larger quadrupole moment of **4** in the excited state than that of **1**, which is reasonable considering the significant electron-donating property of Ph_2N group. It is beyond our expectation that the slopes of **5** and **6** are even a little steeper than that of **4** (slope = 10453 cm^{-1} for **5** and 11671 cm^{-1} for **6**). This may be ascribed to their localized HOMO contributed from only one (diphenylamino)-phenyl moiety, which results in a dipole moment rather than a quadrupole moment. These results suggest that the emissions

Table 2. UV/Vis Absorption and Fluorescence Data of Boryl-Substituted *p*-Quaterphenyls 1 and 4−6 in Various Solvents

		$\Lambda_{abs}{}^{a}$ (nm)	$\lambda_{em}{}^{b}$ (nm)	$\Delta\nu^{c}$ (cm^{-1})
1	cyclohexane	287	449	12571
	benzene	290	441	11807
	$CHCl_3$	289	451	12429
	THF	290	454	12456
	MeCN	289	459	12815
4	cyclohexane	379^{d}	457	4503
	benzene	384^{d}	469	4719
	$CHCl_3$	374^{d}	480	5904
	THF	381^{d}	493	5962
	MeCN	380^{d}	529	7412
5	cyclohexane	300	433	10238
	benzene	301	449	10950
	$CHCl_3$	303	458	11169
	THF	299	470	12168
	MeCN	295	506	14135
6	cyclohexane	300	445	10861
	benzene	301	448	10901
	$CHCl_3$	303	459	11216
	THF	300	478	12412
	MeCN	298	538	14969

[a] Only the longest absorption maximum wavelengths are given. [b] Excited at the longest absorption maxima. [c] Stokes shift. [d] Observed as shoulder.

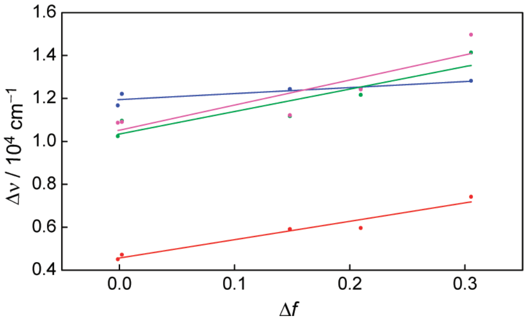

Figure 5. Lippert−Mataga plots for boryl-substituted *p*-quaterphenyls **1** (blue), **4** (red), **5** (green), **6** (magenta).

of all these molecules come from the highly polarized excited states induced by the intramolecular CT transition, irrespective of their different substitution patterns. The intramolecular CT transition generally leads to the large Stokes shift, which is supposed to facilitate suppressing the fluorescence quenching in the solid state.

$$\Delta\nu = \nu_{\mathrm{A}} - \nu_{\mathrm{F}} = \frac{2\Delta f}{\mathrm{hca}^3}(\mu_{\mathrm{e}} - \mu_{\mathrm{g}})^2 + C \tag{1}$$

$$\Delta f = \frac{\varepsilon - 1}{2\varepsilon + 1} - \frac{n^2 - 1}{2n^2 + 1} \tag{2}$$

Photophysical Properties in the Solid State. It is intriguing to note that all these boryl-substituted *p*-quaterphenyls **1**−**6** exhibit bright blue fluorescence even in the powder form. This observation prompted us to investigate their photophysical properties in the solid state in details. Thin films of compounds **1**−**6** were prepared from their dichloromethane solutions with ca. 3 mg mL^{-1} concentration on the quartz plates and their absorption and fluorescence spectra were directly measured. The absolute fluorescence quantum yields were determined by a calibrated integrating sphere system. The corresponding spectra are shown in Figure 6, and the data are summarized in Table 3.

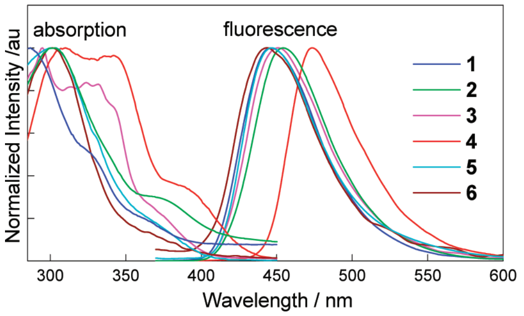

Figure 6. Absorption and fluorescence spectra of boryl-substituted *p*-quaterphenyls **1**−**6** in the spin-coated films.

Table 3. UV/Vis Absorption and Fluorescence Data for Boryl-Substituted *p*-Quaterphenyls 1−6 in the Spin-Coated Films

	absorption	fluorescence	
	λ_{abs}[a] (nm)	λ_{em}[b] (nm)	Φ_{F}[b]
1	287	446	0.94
2	373 (sh)	454	0.99
3	370 (sh)	447	0.83
4	391 (sh)	473	0.99
5	304	444	0.72
6	301	446	0.60

[a] Only the longest maxima are shown. [b] Excited at the longest absorption maxima. [c] Absolute quantum yields determined by a calibrated integrating sphere system.

In the absorption and fluorescence spectra, compounds **1**−**6** maintain almost the same spectra as those in benzene solutions, in terms of the maximum wavelengths as well as the full width at the half-maximum (fwhm) (Supporting Information). These results suggest the formation of neither aggregates in the ground state nor an excimer in the excited state. The lateral boryl group is bulky enough to prevent the intermolecular interactions in the solid state. Another noticeable characteristic for this series of *π*-conjugated molecules is that they show the increased fluorescence intensities in the solid-state compared with those in benzene solutions. Such fluorescence behavior may be ascribed to the easily exchangeable multiple conformations of the nonplanar structure of the main chain, which facilitate the nonradiative decay of the excited state. In the solid-state, the exchanges between multiple conformations are greatly suppressed due to the spatial congestion of the molecular stacking in the solid-state.[8] It is most noteworthy that all the *p*-quaterphenyl derivatives display an intense fluorescence with good to excellent quantum yields (Φ_{F} = 0.60−0.99) for their spin-coated films, even for **5** and **6**, the quantum yields of which in benzene are very low. The high fluorescence efficiency in the solid state is presumably attributed to the absence of the intermolecular interaction in the solid state, as well as the large Stokes shift induced by the intramolecular CT transition.[13−15] In addition, the emission bands of **1**−**6** are in the blue light region with the maxima ranging from 446 to 473 nm. Moreover, compounds **3**−**6** not only display intense blue fluorescence in the solid state, but also contain both electron-accepting boryl group and electron-donating carbazolyl or diphenylamino group, which may make them potentially applied as bipolar blue emitters in OLEDs. Bipolar light-emitting materials would facilitate exciton formation (via stable cation and anion radicals) and may improve charge balancing in OLEDs.[21]

Thermal Properties. Considering the excellent quantum yields of the current *p*-quaterphenyls in the spin-coated films, we evaluated their thermal stabilities by thermogravimetric analysis (TGA) and differential scanning calorimetry (DSC) to explore their potential utility as the blue emitters in OLEDs using **3** and **4** as the representative molecules. The melting points of **3** and **4** measured by DSC are 323 and 267 °C, respectively. Although both compounds showed no mesophase or glass transition, they displayed very high decomposition temperatures. The decomposition temperatures for a 5% weight loss (T_{d5}) of **3** and **4** are 437 and 429 °C, respectively. The thermal analyses indicate that these two compounds exhibit excellent thermal stability, which ensures that they are stable and suitable for the vacuum deposition in the fabrication of OLEDs.

Electrochemical Properties. To further evaluate the potential applicability of the present boryl-substituted *p*-quaterphenyl system in electronic devices, we also investigated the electrochemical properties of **3** and **4** by cyclic voltammetry (CV), which are shown in Figure 7. Both compounds show not only reversible oxidation waves (**3**: +0.57, +0.88 V; **4**: +0.48 V, versus ferrocene/ferrocenium ($\mathrm{Fc/Fc^+}$)), but also reversible

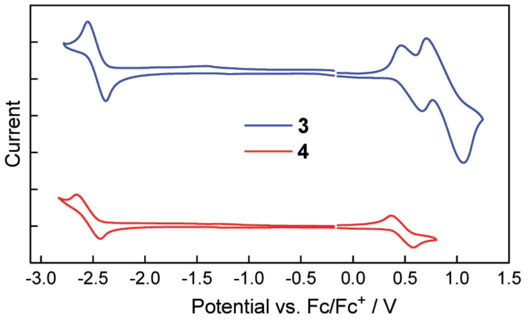

Figure 7. Cyclic voltammograms of **3** and **4** in THF (1 mM), measured with TBAP (0.1 M) as the supporting electrolyte at a scan rate of 100 mV/s.

reduction waves (**3**: −2.46 V; **4**: −2.54 V). The high reversibility in their redox process demonstrates the substantial stability of the produced species, and is indicative of their potential use as bipolar transporting blue emitters. Our current molecular design may provide an efficient strategy to achieve solid-state blue emissive materials with bipolar transporting properties, which is of great interest for realizing full-color display of OLEDs.

■ CONCLUSIONS

We have designed and synthesized a series of *p*-quaterphenyls **1**−**6** laterally substituted with a boryl group. This series of boryl-substituted *p*-quaterphenyls were facilely prepared by Pd(0)-catalyzed Suzuki−Miyaura cross-coupling reaction from a common precursor. And thus further functionalization was easily realized by introducing various electron-donating groups at different substitution sites. Owing to the influence of steric bulkiness and the electron-accepting property of the lateral dimesitylboryl group, these quaterphenyls exhibit a twisted main-chain structure and efficient intramolecular charge-transfer transition with a large Stokes shift, facilitating the suppression of fluorescence quenching in the solid-state. All of these compounds display intense fluorescence in the solid state with good to excellent quantum yields in the blue region, even those derivatives **3**−**6** containing both the electron-accepting boryl group and the electron-donating carbazolyl or diphenylamino group. In addition, the two representative compounds **3** and **4** possess high thermal stability and good oxidation−reduction reversibility, which together with their excellent solid state fluorescence efficiency make them promising bipolar transporting blue emitters. We here not only disclosed a new kind of emissive materials, but also demonstrated the general utility of the molecular design to obtain organic emissive solids by introduction of bulky electron-accepting boryl group at the side position of electron-donating framework.[13] The preliminary results will provide a firm direction for rational design of such kind of materials. Further application of these obtained blue emissive materials to OLEDs is in progress.

■ EXPERIMENTAL SECTION

General Methods. All reactions were carried out under nitrogen atmosphere. Compound 7 was prepared according to the literature.[17]

Computational Methods. All calculations were conducted by using the Gaussian 09 program.[22]

4,4′-Dibromo-2-(dimesitylboryl)biphenyl (8). To a solution of 4,4′-dibromo-2-iodobiphenyl 7 (3.54 g, 8.0 mmol) in anhydrous THF (20 mL) was added a hexane solution of *n*-BuLi (5.0 mL, 1.6 M, 8.0 mmol) dropwise by syringe at −78 °C. The mixture was stirred at the same temperature for 1 h. A solution of dimesitylboron fluoride (6.43 g, 24 mmol) in anhydrous THF (10 mL) was added to the reaction mixture via syringe. The reaction mixture was warmed to room temperature and stirred overnight. The reaction was quenched with saturated solution of NaCl, and the aqueous layer was extracted with CH_2Cl_2. The combined organic layer was dried over anhydrous Na_2SO_4, filtered, and concentrated under reduced pressure. The resulting mixture was subjected to a silica gel column chromatography (petroleum ether, R_f = 0.20) to afford 2.30 g (4.1 mmol) of **8** in 51% yield as a pale yellow solid: mp 139−141 °C; ^{1}H NMR ($CDCl_3$, 300 MHz) 7.58 (dd, *J* = 8.1, 1.8 Hz, 1H), 7.51 (d, *J* = 1.8 Hz, 1H), 7.15 (d, *J* = 8.1 Hz, 1H), 7.08 (d, *J* = 8.1 Hz, 2H), 6.88 (d, *J* = 8.1 Hz, 2H), 6.61 (s, 4H), 2.21 (s, 6H), 1.91 (s, 12H); ^{13}C NMR($CDCl_3$, 75 MHz) δ 145.3, 140.9, 140.8, 139.7, 138.7, 136.9, 133.1, 130.6, 129.4, 128.8, 129.3, 127.8, 121.6, 120.5, 22.8, 20.6. Anal. Calcd for $C_{30}H_{29}BBr_2$: C, 64.32; H, 5.21. Found: C, 64.41; H, 5.29.

3′′-Dimesitylboryl-[1,1′:4′,1′′:4′′,1′′′]quaterphenyl (1). To a mixture of **8** (112 mg, 0.2 mmol), phenylboronic acid (73 mg, 0.6 mmol), and $Pd(PPh_3)_4$ (12 mg, 0.01 mmol) were added degassed toluene (20 mL) and aqueous sodium carbonate solution (2 M, 2 mL) under a stream of nitrogen. The reaction mixture was stirred and refluxed at 110 °C overnight. The mixture was cooled to room temperature and then extracted with CH_2Cl_2. The combined organic layer was dried over anhydrous Na_2SO_4, filtered, and concentrated under reduced pressure. The resulting mixture was subjected to a silica gel column chromatography (5/1 petroleum ether/CH_2Cl_2, *Rf* = 0.32) to give 107 mg (0.19 mmol) of **1** in 96% yield as a colorless solid: mp 183−185 °C; ^{1}H NMR ($CDCl_3$, 300 MHz) δ 7.72 (dd, *J* = 8.1, 1.8 Hz, 1H), 7.69 (d, *J* = 1.8 Hz, 1H), 7.52 (d, *J* = 7.2 Hz, 2H), 7.47 (d, *J* = 8.1 Hz, 1H), 7.38−7.43 (m, 6H), 7.29−7.34 (m, 2H), 7.18−7.24(m, 4H), 6.58 (s, 4H), 2.14 (s, 6H), 1.97 (s, 12H); ^{13}C NMR ($CDCl_3$, 75 MHz) δ 147.3, 146.8, 142.2, 142.0, 140.9, 140.4, 139.8, 139.1, 138.9, 138.0, 133.5, 129.4, 129.0, 128.5, 128.2, 128.0, 127.6, 126.6, 126.6, 126.4, 125.3, 22.8, 20.6; HRMS (ESI) 593.2779 ([M + K]$^+$), calcd for $C_{42}H_{39}BK$ 593.2782.

4,4′′′-Dimethoxy-2′′-dimesitylboryl-[1,1′:4′,1′′:4′′,1′′′]-quaterphenyl (2). This compound was prepared essentially in the same manner as described for **1** using **8** (224 mg, 0.4 mmol) and 4-methoxylphenylboronic acid (182 mg, 1.2 mmol), $Pd(PPh_3)_4$ (23 mg, 0.02 mmol), degassed toluene (20 mL), and aqueous sodium carbonate solution (2 mL, 2 M). The purification by a silica gel column chromatography (4/1 petroleum ether/CH_2Cl_2, R_f = 0.15) afforded 196 mg (0.32 mmol) of **2** in 80% yield as a colorless solid: mp 225−227 °C; ^{1}H NMR ($CDCl_3$, 300 MHz) δ 7.68 (dd, *J* = 8.1, 1.8 Hz, 1H), 7.63 (d, *J* = 1.8 Hz, 1H), 7.47−7.43 (m, 3H), 7.38 (d, *J* = 8.7 Hz, 2H), 7.20−7.13 (m, 4H), 6.97−6.93 (m, 4H), 6.57 (s, 4H), 3.85 (s, 3H), 3.83(s, 3H), 2.14(s, 6H), 1.97(s, 12H); ^{13}C NMR($CDCl_3$, 75 MHz) δ 158.6, 158.4, 147.2, 146.3,142.2, 141.4, 139.7, 138.6, 138.4, 137.9, 133.5, 133.0, 132.9, 129.3, 128.5, 128.4, 127.6, 127.6, 127.5, 124.9, 113.7, 113.5, 54.87, 54.84, 22.8, 20.6; HRMS (ESI) 653.2954 ([M + K]$^+$), calcd for $C_{44}H_{43}BO_2K$ 653.2993.

4,4′′′-Bis(*N*,*N*-carbazolyl)-2′′-dimesitylboryl-[1,1′:4′,1′′:4′′,1′′′]quaterphenyl (3). This compound was prepared essentially in the same manner as described for **1** using **8** (107 mg, 0.19 mmol) and 4-carbazolylphenylboronic acid (163 mg, 0.57 mmol), $Pd(PPh_3)_4$ (12 mg, 0.01 mmol), degassed toluene (20 mL), and aqueous sodium carbonate solution (2 mL, 2 M). The purification by a silica gel column chromatography (4/1 petroleum ether/CH_2Cl_2, R_f = 0.30) afforded 123 mg (0.14 mmol) of **3** in 73% yield as a colorless solid: mp >300 °C; ^{1}H NMR ($CDCl_3$, 300 MHz) δ 8.18−8.14 (m, 4H), 7.86 (dd, *J* = 7.8, 2.1 Hz, 1H), 7.82 (d, *J* = 2.1 Hz, 1H), 7.76 (d, *J* = 8.4 Hz, 2H), 7.69−7.56 (m, 7H), 7.52−7.39 (m, 8H), 7.32−7.27 (m, 8H), 6.65 (s, 4H), 2.20 (s, 6H), 2.04 (s, 12H). ^{13}C NMR ($CDCl_3$, 75 MHz) δ 147.5, 147.0, 142.2, 140.4, 140.3, 139.9, 139.3, 138.3, 138.1, 138.0, 136.4, 136.1, 133.4, 129.6, 129.0, 128.6, 128.0, 127.8, 127.7, 126.8, 126.7, 125.4, 125.3, 122.9, 119.8, 119.5, 109.3, 22.9, 20.6; HRMS (ESI) 883.4353 ([M]$^+$), calcd for $C_{66}H_{53}BN_2$ 883.4302.

3′′-Dimesitylboryl-4,4′′′-bis(*N*,*N*-diphenylamino)-[1,1′:4′,1′′:4′′,1′′′]quaterphenyl (4). This compound was prepared essentially in the same manner as described for **1** using **8** (112 mg, 0.2

mmol) and 4-diphenylaminophenylboronic acid (173 mg, 0.6 mmol), $Pd(PPh_3)_4$ (11 mg, 0.01 mmol), degassed toluene (20 mL), and aqueous sodium carbonate solution (2 mL, 2 M). The purification by a silica gel column chromatography (4/1 petroleum ether/CH_2Cl_2, R_f = 0.37) afforded 130 mg (0.14 mmol) of **4** in 70% yield as bluish green solids: mp 273−275 °C; ^1H NMR ($CDCl_3$, 300 MHz) δ 7.69 (d, J = 7.5 Hz, 1H), 7.66 (s, 1H), 7.44 (d, J = 7.8 Hz, 1H), 7.39 (d, J = 8.1 Hz, 2H), 7.31−6.92 (m, 30H), 6.57 (s, 4H), 2.14 (s, 6H), 1.97 (s, 12H). ^{13}C NMR ($CDCl_3$, 75 MHz) δ 147.2, 147.1, 146.6, 146.4, 146.3, 142.2, 141.5, 139.8, 138.4, 138.3, 137.9, 134.9, 134.1, 132.9, 129.3, 128.7, 128.4, 127.6, 127.2, 124.8, 123.9, 123.3, 123.2, 122.4, 122.3, 22.8, 20.6; HRMS (ESI) 927.4244 ([M + K]$^+$), calcd for $C_{66}H_{57}BN_2K$ 927.4252.

3′′-Dimesitylboryl-2,2′′′-(*N*,*N*-diphenylamino)-[1,1′:4′,1′′:4′′,1′′′]quaterphenyl (5). This compound was prepared essentially in the same manner as described for **1** using **8** (168 mg, 0.3 mmol) and 2-diphenylaminophenylboronic acid (260 mg, 0.9 mmol), $Pd(PPh_3)_4$ (17 mg, 0.015 mmol), degassed toluene (20 mL), and aqueous sodium carbonate solution (2 mL, 2 M). The purification by a silica gel column chromatography (5/1 petroleum ether/CH_2Cl_2, R_f = 0.20) afforded 52 mg (0.058 mmol) of **5** in 19% yield as white solids: mp 210−212 °C; ^1H NMR ($CDCl_3$, 300 MHz) δ 7.41(dd, J = 7.8, 1.8 Hz, 1H), 7.33−7.16 (m, 9H), 7.07−6.96 (m, 10H), 6.86−6.72 (m, 13H), 6.63 (d, J = 8.4 Hz, 2H), 6.49 (s, 4H), 2.15 (s, 6H), 1.76 (s, 12H); ^{13}C NMR ($CDCl_3$, 75 MHz) δ 147.0, 146.9, 145.6, 145.4, 144.3, 144.1, 142.2, 141.3, 140.4, 139.7, 139.6, 137.7, 137.4, 137.1, 135.0, 131.6, 131.1, 130.3, 129.3, 128.7, 128.4, 128.2, 128.1, 128.0, 127.8, 127.4, 127.4, 126.3, 125.3, 124.9, 121.5, 121.4, 120.8, 120.6, 22.7, 20.6; HR-MS (ESI) 927.4272 ([M + K]$^+$), calcd for $C_{66}H_{57}BN_2K$ 927.4252.

3′′-Dimesitylboryl-3,3′′′-(*N*,*N*-diphenylamino)-[1,1′:4′,1′′:4′′,1′′′]quaterphenyl (6). This compound was prepared essentially in the same manner as described for **1** using **8** (168 mg, 0.3 mmol) and 3-diphenylaminophenylboronic acid (260 mg, 0.9 mmol), $Pd(PPh_3)_4$ (34 mg, 0.03 mmol), degassed toluene (20 mL), and aqueous sodium carbonate solution (2 mL, 2 M). The purification by a silica gel column chromatography (4/1 petroleum ether/CH_2Cl_2, R_f = 0.40) afforded 200 mg (0.22 mmol) of **6** in 75% yield as a white solid: mp 113−115 °C; ^1H NMR ($CDCl_3$, 300 MHz) δ 7.57 (dd, J = 8.1, 1.8 Hz, 1H), 7.55 (d, J = 1.8 H, 1H), 7.36 (d, J = 7.8 Hz, 1H), 7.30−7.21 (m, 10H), 7.16−6.98 (m, 22H), 6.50 (s, 4H), 2.10 (s, 6H), 1.89 (s, 12H). ^{13}C NMR ($CDCl_3$, 75 MHz) δ 147.8, 147.6, 147.3, 147.1, 146.7, 142.0, 141.9, 141.4, 139.6, 138.8, 138.6, 137.8, 133.3, 129.1, 128.95, 128.91, 128.77, 128.72, 128.3, 127.5, 125.1, 123.9, 123.8, 122.4, 122.3, 122.2, 121.9, 121.8, 121.7, 120.7, 120.6, 22.7, 20.5; HRMS (ESI) 927.4241 ([M + K]$^+$), calcd for $C_{66}H_{57}BN_2K$ 927.4251.

X-ray Crystal Structure Analysis of Compound 2.[23] Single crystals of **2** suitable for X-ray crystal analysis were obtained by recrystallization from a hexane/CH_2Cl_2 mixed solvent. Intensity data were collected at 293 K on a Bruker single-crystal CCD X-ray diffractometer (APEX II) with Mo Kα radiation (λ = 0.71069 Å) and graphite monochromator. A total of 20264 reflections were measured at a maximum 2θ angle of 55.0°, of which 7859 were independent reflections (R_{int} = 0.0244). The structure was solved by direct methods (SHELXS-97[23]) and refined by full-matrix least-squares methods on F^2 (SHELEXL-97[23]). All non-hydrogen atoms were refined anisotropically and all hydrogen atoms except for those of the disordered solvent molecules were placed using AFIX instructions. The crystal data are as follows: $C_{44}H_{44}BO_2$; FW = 614.59, crystal size 0.25 × 0.23 × 0.19 mm^3, triclinic, *P*-1, a = 8.4643(8) Å, b = 15.5850(14) Å, c = 15.6693(14) Å, V = 2 1746.1(3) Å^3, Z = 2, D_c = 1.169 g cm^{-3}. The refinement converged to R_1 = 0.0608, wR_2 = 0.1769 ($I > 2\sigma(I)$), GOF = 1.085.

Electrochemical Measurements. Cyclic voltammetry (CV) was performed using a BSA 100W instrument with a scan rate of 100 mV/s. A three-electrode configuration was used for the measurements: a platinum electrode as the working electrode, a platinum wire as the counter electrode, and an Ag/Ag$^+$ electrode as the reference electrode. A 0.1 M solution of tetrabutylammonium perchlorate (TBAP) in THF was used as the supporting electrolyte. The ferrocene/ferrocenium (Fc/Fc$^+$) couple was used as the internal standard.

■ ASSOCIATED CONTENT

Ⓢ Supporting Information

^1H NMR and ^{13}C NMR spectra of all new compounds, absorption and fluorescence spectra of **1−6** in benzene and the solid state, ORTEP drawing of **2**, Cartesian coordinates and total energies for the optimized structures, and crystallographic data of **2** (CIF). These materials are available free of charge via the Internet at http://pubs.acs.org.

■ AUTHOR INFORMATION

Corresponding Author

*E-mail: chzhao@sdu.edu.cn.

Notes

The authors declare no competing financial interest.

■ ACKNOWLEDGMENTS

We are grateful for financial support from the National Nature Science Foundation of China (Grant Nos. 21072117 and 20802041), Nature Science Foundation of Shandong Province (No. Q2008B02), and Science Foundation of the Ministry of Education of China (No. 200804221009).

■ REFERENCES

(1) Tang, C. W.; VanSlyke, S. A. *Appl. Phys. Lett.* **1987**, *51*, 913−915.

(2) (a) Grimsdale, A. C.; Chan, K. L.; Martin, R. E.; Jokisz, P. G.; Holmes, A. B. *Chem. Rev.* **2009**, *109*, 897−1091. (b) Kakafi, Z. H. *Organic Electroluminescence*; CRC Press: New York, 2005. (c) Müllen, K.; Scherf, U. *Organic Light-Emitting Devices*; Wiley-VCH; Weinheim, 2006. (d) Li, Z.; Meng, H. *Organic Light-Emitting Materials and Devices*; CRC Press: Boca Raton, 2006.

(3) (a) Kamtekar, K. T.; Monkman, A. P.; Bryce, M. R. *Adv. Mater.* **2010**, *22*, 572−582. (b) Beaupré, S.; Boudreault, P.-L. T.; Leclerc, M. *Adv. Mater.* **2010**, *22*, E6−E27.

(4) For reviews of emissive organic solids, see: Shimizu, M.; Hiyama, T. *Chem. Asian J.* **2010**, *5*, 1516−1531.

(5) (a) Gaal, M.; List, E. J. W.; Scherf, U. *Macromolecules* **2003**, *36*, 4236−4237. (b) Zhang, H.; Guo, E.; Fang, Y. J.; Ren, P. H.; Yang, W. J. *J. Polym. Sci. Part A: Polym. Chem.* **2009**, *47*, 5488−5497. (c) Yan, W.; Wang, Q.; Lin, Q.; Li, M.; Petersen, J. L.; Shi, X. *Chem.—Eur. J.* **2011**, *17*, 5011−5018.

(6) (a) Qin, T.; Zhou, G.; Scheiber, H.; Bauer, R. E.; Baumgarten, M.; Anson, C. E.; List, E. J. W.; Müllen, K. *Angew. Chem., Int. Ed.* **2008**, *47*, 8292−8296. (b) Wang, J.; Zhao, Y.; Dou, C.; Sun, H.; Xu, P.; Ye, K.; Zhang, J.; Jiang, S.; Li, F.; Wang, Y. *J. Phys. Chem. B* **2007**, *111*, 5082−5089. (c) Sanji, T.; Kanzawa, T.; Tanaka, M. *J. Organomet. Chem.* **2007**, *692*, 5053−5059. (d) Langhals, H.; Krotz, O.; Polborn, K.; Mayer, P. *Angew. Chem., Int. Ed.* **2005**, *44*, 2427−2428. (e) Sato, T.; Jiang, D.-L.; Aida, T. *J. Am. Chem. Soc.* **1999**, *121*, 10658−10659.

(7) Xie, Z.; Yang, B.; Li, F.; Cheng, G.; Liu, L.; Yang, G.; Xu, H.; Ye, L.; Hanif, M.; Liu, S.; Ma, D.; Ma, Y. *J. Am. Chem. Soc.* **2005**, *127*, 14152−14153.

(8) (a) Liu, Y.; Deng, C.; Tang, L.; Qin, A.; Hu, R.; Sun, J. Z.; Tang, B. Z. *J. Am. Chem. Soc.* **2011**, *133*, 660−663. (b) Yuan, W. Z.; Chen, S.; Lam, J. W. Y.; Deng, C.; Lu, P.; Sung, H. H.-Y.; Williams, I. D.; Kwok, H. S.; Zhang, Y.; Tang, B. Z. *Chem. Commun.* **2011**, *47*, 11216−11218. (c) Zhao, Z.; Wang, Z.; Lu, P.; Chan, C. Y. K.; Liu, D.; Lam, J. W. Y.; Sung, H. H. Y.; Williams, I. D.; Ma, Y.; Tang, B. *Angew. Chem., Int. Ed.* **2009**, *48*, 7608−7611. (d) Dong, Y.; Lam, J. W. Y.; Qin, A.; Sun, J.; Liu, J.; Li, Z.; Sun, J.; Sung, H. H. Y.; Williams, I. D.; Kwok, H. S.; Tang, B. Z. *Chem. Commun.* **2007**, *43*, 3255−3257. (e) Tong, H.; Hong, Y.; Dong, Y.; Häußler, M.; Lam, J. W. L.; Li, Z.; Guo, Z.; Tang, B. Z. *Chem. Commun.* **2006**, *42*, 3705−3707. (f) Yu, G.; Yin, S.; Liu, Y.; Chen, J.; Xu, X.; Sun, X.; Ma, D.; Zhan, X.; Peng, Q.; Shuai, Z.; Tang, B.; Zhu, D.; Fang, W.; Luo, Y. *J. Am. Chem. Soc.* **2005**, *127*, 6335−6346. (g) Luo, J.; Xie, Z.; Lam, J. W. Y.; Cheng, L.; Chen, H.;

Qiu, C.; Kwok, H. S.; Zhan, X.; Liu, Y.; Zhu, D.; Tang, B. Z. *Chem. Commun.* **2001**, *37*, 1740−1741.

(9) (a) Zhang, Z.; Xu, B.; Su, J.; Shen, L.; Xie, Y.; Tian, H. *Angew. Chem., Int. Ed.* **2011**, *50*, 11654−11657. (b) Wang, B.; Wang, Y.; Hua, J.; Jiang, Y.; Huang, J.; Qian, S.; Tian, H. *Chem.—Eur. J.* **2011**, *17*, 2647−2655. (c) Ning, Z.; Chen, Z.; Zhang, Q.; Yan, Y.; Qian, S.; Cao, Y.; Tian, H. *Adv. Funct. Mater.* **2007**, *17*, 3799−3807.

(10) (a) Kim, S.; Zheng, Q.; He, G. S.; Bharali, D. J.; Pudavar, H. E.; Baev, A.; Prasad, P. N. *Adv. Funct. Mater.* **2006**, *16*, 2317−2323. (b) Itami, K.; Ohashi, Y.; Yoshida, J. *J. Org. Chem.* **2005**, *70*, 2778−2792. (c) An, B.-K.; Kwon, S.-K.; Jung, S. D.; Park, S. Y. *J. Am. Chem. Soc.* **2002**, *124*, 14410−14415.

(11) (a) Würthner, F.; Kaiser, T. E.; Saha-Möller, C. R. *Angew. Chem., Int. Ed.* **2011**, *50*, 3376−3410. (b) Kaiser, T. E.; Wang, H.; Stepanenko, V.; Würthner, F. *Angew. Chem., Int. Ed.* **2007**, *46*, 5541−5544.

(12) (a) Saragi, T. P. I; Spehr, T.; Siebert, A.; Fuhrmann-Lieker, T.; Salbeck, J. *Chem. Rev.* **2007**, *107*, 1011−1065. (b) Poriel, C.; Cocherel, N.; Rault-Berthelot, J.; Vignau, L.; Jeannin, O. *Chem.—Eur. J.* **2011**, *17*, 12631−12645. (c) Thirion, D.; Rault-Berthelot, J.; Vignau, L.; Poriel, C. *Org. Lett.* **2011**, *13*, 4418−4421. (d) Wang, J.; Wan, W.; Jiang, H.; Gao, Y.; Jiang, X.; Lin, H.; Zhao, W.; Hao, J. *Org. Lett.* **2010**, *12*, 3874−3877.

(13) (a) Zhao, C.-H.; Wakamiya, A.; Inukai, Y.; Yamaguchi, S. *J. Am. Chem. Soc.* **2006**, *128*, 15934−15935. (b) Wakamiya, A.; Mori, K.; Yamaguchi, S. *Angew. Chem., Int. Ed.* **2007**, *46*, 4273−4276. (c) Zhao, C.-H.; Wakamiya, A.; Yamaguchi, S. *Macromolecules* **2007**, *40*, 3898−3900. (d) Zhao, C.-H.; Sakuda, E.; Wakamiya, A.; Yamaguchi, S. *Chem.—Eur. J.* **2009**, *15*, 10603−10612.

(14) Shimizu, M.; Takeda, Y.; Higashi, M.; Hiyama, T. *Angew. Chem., Int. Ed.* **2009**, *48*, 3653−3656.

(15) Zhao, C.-H.; Zhao, Y.-H.; Pan, H.; Fu, G.-L. *Chem. Commun.* **2011**, *47*, 5518−5520.

(16) Recent reviews for boron-based π-electron materials: (a) Wade, C. R.; Broomsgrove, A. E. J.; Aldridge, S.; Gabbaï, F. P. *Chem. Rev.* **2010**, *110*, 3958−3984. (b) Jäkle, F. *Chem. Rev.* **2010**, *110*, 3985−4022. (c) Hudnall, T. W.; Chiu, C.-W.; Gabbaï, F. P. *Acc. Chem. Res.* **2009**, *42*, 388−397. (d) Hudson, Z. M.; Wang, S. *Acc. Chem. Res.* **2009**, *42*, 1584−1596. (e) Yamaguchi, S.; Wakamiya, A. *Pure Appl. Chem.* **2006**, *78*, 1413−1424. (f) Entwistle, C. D.; Marder, T. B. *Chem. Mater.* **2004**, *16*, 4574−4585. (g) Entwistle, C. D.; Marder, T. B. *Angew. Chem., Int. Ed.* **2002**, *41*, 2927−2931.

(17) Chi, C.-C.; Chiang, C.-L.; Liu, S.-W.; Yueh, H.; Chen, C.-T.; Chen, C.-T. *J. Mater. Chem.* **2009**, *19*, 5561−5571.

(18) (a) Zhou, G.; Ho, C.-L.; Wong, W.-Y.; Wang, Q.; Ma, D.; Wang, L.; Lin, Z.; Marder, T. B.; Beeby, A. *Adv. Funct. Mater.* **2008**, *18*, 499−511. (b) Bai, D.-R.; Liu, X.-Y.; Wang, S. *Chem.—Eur. J.* **2007**, *13*, 5713−5723. (c) Liu, X. Y.; Bai, D. R.; Wang, S. *Angew. Chem., Int. Ed.* **2006**, *45*, 5475−5478. (d) Sun, Y.; Wang, S. *Inorg. Chem.* **2010**, *49*, 4394−4404. (e) Wakamiya, A.; Taniguchi, T.; Yamaguchi, S. *Angew. Chem., Int. Ed.* **2006**, *45*, 3170−3173. (f) Wakamiya, A.; Mishima, K.; Ekawa, K.; Yamaguchi, S. *Chem. Commun.* **2008**, *44*, 579−581.

(19) Wang, N.; Hudson, Z. M.; Wang, S. *Organometallics* **2010**, *29*, 4007−4011.

(20) (a) Strehmel, B.; Sarker, A. M.; Malpert, J. H.; Strehmel, V.; Seifert, H.; Neckers, D. C. *J. Am. Chem. Soc.* **1999**, *121*, 1226−1236. (b) Krebs, F. C.; Spanggaard, H. *J. Org. Chem.* **2002**, *67*, 7185−7192.

(21) (a) Shirota, Y.; Kinoshita, M.; Noda, T.; Okumoto, K.; Ohara, T. *J. Am. Chem. Soc.* **2000**, *122*, 11021−11022. (b) Huang, T.-H.; Lin, J. T.; Chen, L.-Y.; Lin, Y.-T.; Wu, C.-C. *Adv. Mater.* **2006**, *18*, 602−606. (c) Kulkarni, A. P.; Kong, X.; Jenekhe, S. A. *Adv. Funct. Mater.* **2006**, *16*, 1057−1066. (d) Doi, H.; Kinoshita, M.; Okumoto, K.; Shirota, Y. *Chem. Mater.* **2003**, *15*, 1080−1089.

(22) Gaussian 09, Revision A.02: Frisch, M. J.; Trucks, G. W.; Schlegel, H. B.; Scuseria, G. E.; Robb, M. A.; Cheeseman, J. R.; Scalmani, G.; Barone, V.; Mennucci, B.; Petersson, G. A.; Nakatsuji, H.; Caricato, M.; Li, X.; Hratchian, H. P.; Izmaylov, A. F.; Bloino, J.; Zheng, G.; Sonnenberg, J. L.; Hada, M.; Ehara, M.; Toyota, K.; Fukuda, R.; Hasegawa, J.; Ishida, M.; Nakajima, T.; Honda, Y.; Kitao, O.; Nakai, H.; Vreven, T.; Montgomery, J. A., Jr.; Peralta, J. E.; Ogliaro, F.; Bearpark, M.; Heyd, J. J.; Brothers, E.; Kudin, K. N.; Staroverov, V. N.; Kobayashi, R.; Normand, J.; Raghavachari, K.; Rendell, A.; Burant, J. C.; Iyengar, S. S.; Tomasi, J.; Cossi, M.; Rega, N.; Millam, J. M.; Klene, M.; Knox, J. E.; Cross, J. B.; Bakken, V.; Adamo, C.; Jaramillo, J.; Gomperts, R.; Stratmann, R. E.; Yazyev, O.; Austin, A. J.; Cammi, R.; Pomelli, C.; Ochterski, J. W.; Martin, R. L.; Morokuma, K.; Zakrzewski, V. G. ; Voth, G. A.; Salvador, P.; Dannenberg, J. J.; Dapprich, S.; Daniels, A. D.; Farkas, O.; Foresman, J. B.; Ortiz, J. V.; Cioslowski, J.; Fox, D. J. Gaussian, Inc., Wallingford, CT, 2009.

(23) Sheldrick, G. M. *SHELX-97, Program for the Refinement of Crystal Structures*; University of Gottingen: Gottingen, Germany, 1997.